

Hydraulic jumps on shear flows with constant vorticity

Henrik Kalisch*, Vincent Teyekpiti

Department of Mathematics, University of Bergen, Bergen, Norway

ARTICLE INFO

Article history:

Received 3 April 2018

Received in revised form 5 July 2018

Accepted 10 August 2018

Available online 18 August 2018

ABSTRACT

In this work, the influence of constant background vorticity on the properties of shock waves in a shallow water system are considered. It is shown that the flow-depth ratio of stationary shocks can be written as a function of two non-dimensional parameters: the Froude number, suitably defined in the presence of the shear flow, and a non-dimensional vorticity. Some properties of these hydraulic jumps are explored, and it is shown that stronger background vorticity has the effect of moderating the strength of the hydraulic jump.

© 2018 Elsevier Masson SAS. All rights reserved.

1. Introduction

Modeling of surface wave motion in a fluid is normally based on classical systems which are obtained in the framework of irrotational flow. In such a context, the influence of vorticity is completely disregarded in the formulation of the governing equations. Although this consideration is justified in many circumstances, there are also a fair number of observed cases in near-shore hydrodynamics and open channel flow where this approach is unsuitable.

Indeed, there is ample evidence that vorticity may have a large impact on wave motion in a variety of situations. For example, it was recently shown that vorticity has significant influence on the modulational stability of quasi-periodic wavetrains [1,2] as well as the streamline pattern and pressure profiles in long waves [3–8]. The importance of vorticity in the modeling of free surface waves has also been exhibited in recent studies of wave–current interaction [9], the interaction of point vortices and vortex patches with the free surface [10,11], the influence of non-constant vorticity on small amplitude waves [12] and the creation of vorticity in long-wave models [13].

In the current work, we are concerned with the interaction of surface waves with an existing shear current. Such currents are created by the action of wind stress at the free surface and viscous stress at the bed, as well as tidal forcing. Once established, these shear currents may be taken as background conditions when studying individual surface waves. For example, the time scales needed to create such currents through wind forcing are typically much larger than the typical interaction time of a single wave with such a current. Moreover, on small time scales, surface waves are

relatively unaffected by viscosity, so that an inviscid theory may be used.

In order to avoid undue mathematical complexity, it is assumed that the long waves to be described are perturbations of an existing background flow with a linear shear profile. This approach has been used by a number of authors (see for example [6,14–19]), and it has been indicated to approximate naturally occurring shear flows fairly well [20]. In particular, it was shown in [21] that the dispersion relation associated with a linear background shear gives rather good agreement with experimentally measured dispersion relation. It was also argued in [5] that linear shear flows can be used as a first approximation to more general shear profiles in the long-wave regime since the wavelength of the waves is then on a different scale than the variation of the shear profile.

Very recently, a new shallow-water system incorporating constant background shear has been found independently in [22–24]. Supposing a background shear flow of the form $U(z) = \Gamma z$, the system is written in terms of the total flow depth H and horizontal velocity perturbation u as

$$H_t + \left(\frac{\Gamma}{2}H^2 + uH\right)_x = 0, \quad (1.1)$$

$$\left(\frac{\Gamma}{2}H^2 + uH\right)_t + \left(\frac{\Gamma^2}{3}H^3 + \Gamma uH^2 + u^2H + \frac{1}{2}gH^2\right)_x = 0. \quad (1.2)$$

The first of these equations describes mass conservation, and the second arises from momentum conservation.

In the present contribution, this new system is used to understand the influence of vorticity on the properties of hydraulic jumps. An analysis of shock-wave solutions of the system (1.1), (1.2) detailed in the body of this paper shows that stationary jumps can be described in terms of two non-dimensional numbers, one being the Froude number, and the other incorporating the background vorticity Γ . To be more precise, if H_L is the upstream flow depth and u_L is the fluid velocity upstream of a stationary

* Corresponding author.

E-mail addresses: henrik.kalisch@math.uib.no (H. Kalisch), vincent.teyekpiti@math.uib.no (V. Teyekpiti).

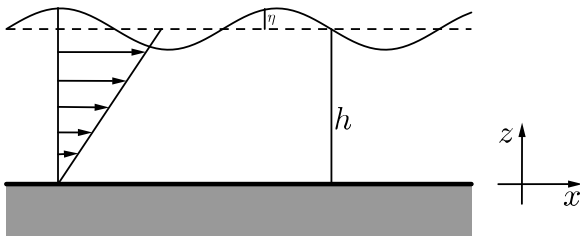


Fig. 1. Schematic representation of a linear shear flow over an even bottom.

jump, we define the Froude number by

$$Fr = \frac{u_L + \Gamma/2}{\sqrt{gH_L}},$$

and the non-dimensional vorticity by

$$\Omega = \frac{\Gamma^2 H}{6g},$$

where g is the gravitational constant, and the factor 6 is chosen for the sake of reaching a tidy expression in the final relation. These two parameters completely determine the strength of the jump, which is described mathematically as the ratio $\alpha = H_R/H_L$ through the cubic equation

$$\Omega \alpha^3 + (1 + \Omega) \alpha^2 + (1 + \Omega) \alpha - 2Fr_L^2 = 0.$$

The derivation of this equation will be given in Section 4.

Our work is motivated in part by [25], where hydraulic jumps were studied in the presence of variable vorticity. This paper made an important contribution in the understanding of hydraulic jumps as transient phenomena, and the authors of [25] were the first to be able to simulate oscillation of the jump toe in a physically reasonable way, obtaining a very close match with experimental data. While hydraulic jumps are classically compartmentalized using the Froude number, one of the findings of [25] was that a hydraulic jump does not simply depend on a single parameter, the upstream Froude number, but also on the vorticity in the flow. In the current work, we study hydraulic jumps using the simplifying assumption of constant background shear. While our model is not able to explain the creation of vorticity in a hydraulic jump which featured prominently in [25], we are able to quantify the dependence of the strength of the hydraulic jump on the vorticity, and give fairly simple closed-form solutions which we hope will prove useful in practical studies investigating the influence of background shear on the properties of hydraulic jumps.

A schematic representation of the problem setup is shown in Fig. 1 where a channel of unit width and even bottom containing a fluid with undisturbed depth h is considered. The elevation of the free surface from its rest state is given by $\eta(x, t)$ so that the total depth at a point x and time t is given by $H(x, t) = h + \eta(x, t)$. The average horizontal velocity is denoted by $u(x, t)$ and the total velocity component is

$$v(x, t, z) \equiv U(z) + u(x, t) = \Gamma z + u, \tag{1.3}$$

where $U(z)$ is the linear shear current and Γ is constant. As shown in [22–24], if the waves at the free surface are long enough compared to the fluid depth h , the appropriate equations describing the shear flow are given by (1.1) and (1.2). If the flow variables are smooth so that the solutions are also smooth, then an equivalent system has the form

$$\partial_t H + \partial_x \left(\frac{\Gamma}{2} H^2 + uH \right) = 0, \tag{1.4}$$

$$\partial_t u + \partial_x \left(\frac{1}{2} u^2 + gH \right) = 0. \tag{1.5}$$

It is well known that in the case of discontinuous solutions, mass and momentum conservation could introduce a Rankine–Hugoniot deficit in (1.5) which may raise an argument against the use of (1.4)–(1.5) in favor of the system (1.1)–(1.2). However, (1.4)–(1.5) is mathematically interesting and the theory contributing to the progress of this system is fully elaborated and the Riemann problem and the initial value problem for this system can be resolved adequately [26–28]. An analysis of these systems in the case of zero vorticity is neatly presented in [29] where it is shown that the combination of discontinuous free-surface solutions and bottom step transitions naturally lead to singular solutions featuring a Rankine–Hugoniot deficit. While the Eqs. (1.1) and (1.2) were found in the works [22–24], these authors did not consider the total mechanical energy equation which must be considered in order to provide a physical selection criterion on the admissibility of shock waves. In the current work, we derive the energy equations and use it to discard non-admissible shocks. As will be shown in Section 2, energy conservation for the shear flow is formulated as

$$\left(\frac{\Gamma}{2} uH^2 + \frac{\Gamma^2}{6} H^3 + \frac{1}{2} u^2 H + \frac{1}{2} gH^2 \right)_t + \left(\frac{3\Gamma}{4} u^2 H^2 + \frac{\Gamma}{2} gH^3 + \frac{\Gamma^2}{2} uH^3 + \frac{\Gamma^3}{8} H^4 + \frac{1}{2} u^3 H + guH^2 \right)_x = 0. \tag{1.6}$$

The plan of the paper is as follows: In Section 2, we formulate the free surface problem for a shear flow over a flat bottom. The derivation is based on the Euler equations for an incompressible and inviscid fluid. In Section 3, the equations are analyzed and mathematical properties of the flow variables are presented. Explicit expressions representing mass conservation and momentum conservation are obtained and it is shown that a shallow water flow over a flat bed in the presence of a linear shear current features energy loss. In Section 4, we explain how to construct a steady state solution for the linear shear flow by defining the Froude number in terms of a depth-averaged integral.

2. Linear shear flow over flat bottom topography

The governing shallow water equations that describe the motion of incompressible and inviscid fluid are derived in this section. We consider a flat-bottom channel with uniform width and set the x -coordinate in the flow direction whilst the z -coordinate is vertically upwards.

Consider a control volume of unit width enclosed by the flat bottom, the free surface and the interval $[x_1, x_2]$ such that $x_1 < x_2$ on the lateral sides. The mass of the incompressible, inviscid fluid of uniform depth contained in the control volume is

$$\mathcal{M} = \int_{x_1}^{x_2} \int_0^{H(x,t)} \rho \, dz \, dx.$$

If the free surface and the flat bottom are impermeable so that no transfer of mass occur there, then the physical hypothesis of mass conservation requires that the rate of change of mass per unit time is proportional to the mass flux through the lateral boundaries. The mathematical idealization of this concept is expressed by the integral equation

$$\begin{aligned} \frac{d}{dt} \int_{x_1}^{x_2} \int_0^{H(x,t)} \rho \, dz \, dx \\ = \int_0^{H(x_1,t)} \rho v(x_1, t) \, dz - \int_0^{H(x_2,t)} \rho v(x_2, t) \, dz. \end{aligned}$$

If the flow variables as well as the domain are smooth, then the above equation can be written as

$$\frac{d}{dt} \int_{x_1}^{x_2} \rho H(x, t) \, dx + \left[\int_0^{H(x,t)} \rho (\Gamma z + u(x, t)) \, dz \right]_{x_1}^{x_2} = 0.$$

If we have constant density ρ , we can divide through by $(x_2 - x_1)\rho$. Then by letting $x_2 - x_1 \rightarrow 0$, we see that the integrand must be zero, so that we obtain the equation representing mass conservation in the form

$$\partial_t H + \partial_x \left(\frac{\Gamma}{2} H^2 + uH \right) = 0.$$

In a similar manner, an expression representing momentum conservation in the control volume can be derived. If we suppose that pressure force is the only force acting on the control volume, then conservation of momentum is based on the physical principle that the fluid is in a hydrostatic balance so that the pressure $p = p(x, z, t)$ is introduced. Applying this assumption in a fluid column $[x_1, x_2] \times [z, z + \Delta z]$ gives

$$(p(\bar{x}, z + \Delta z, t) - p(\bar{x}, z, t))(x_2 - x_1) = -(x_2 - x_1)\rho g \Delta z,$$

for $\bar{x} \in [x_1, x_2]$. If the flow variables are smooth, then dividing through by $(x_2 - x_1)\Delta z$ and taking the limit as $\Delta z \rightarrow 0$ gives

$$\frac{dp}{dz} = -\rho g.$$

Integrating and normalizing the pressure to be zero at the surface yields the relation

$$p(x, z, t) = \rho g (H(x, t) - z) \quad (2.1)$$

for the hydrostatic pressure. Considering the control volume described above, the total horizontal momentum in the control volume is

$$\mathcal{I} = \int_{x_1}^{x_2} \int_0^{H(x,t)} \rho v(x, t) dz dx.$$

Momentum conservation is obtained from Newton's second law which requires that the rate of change of total momentum is equal to the net momentum flux through the lateral boundaries plus the pressure forces acting on the boundaries. This is expressed mathematically as

$$\begin{aligned} \frac{d}{dt} \int_{x_1}^{x_2} \int_0^{H(x,t)} \rho v(x, t) dz dx \\ = \int_0^H \rho v^2(x_1, t) dz - \int_0^H \rho v^2(x_2, t) dz \\ + \int_0^H p(x_1, z, t) dz - \int_0^H p(x_2, z, t) dz. \end{aligned}$$

Substituting the total velocity in (1.3) and the pressure term in (2.1) and simplifying yield

$$\begin{aligned} \frac{d}{dt} \int_{x_1}^{x_2} \rho \left[\left(\frac{\Gamma}{2} H^2 + uH \right) \right. \\ \left. + \left(\frac{\Gamma^2}{3} H^3 + \Gamma uH^2 + u^2H + \frac{g}{2} H^2 \right) \right] dx = 0 \end{aligned}$$

Dividing through by $(x_2 - x_1)\rho$ and taking the limit as $(x_2 - x_1) \rightarrow 0$ shows that the momentum conservation equation can be expressed as

$$\left(\frac{\Gamma}{2} H^2 + uH \right)_t + \left(\frac{\Gamma^2}{3} H^3 + \Gamma uH^2 + u^2H + \frac{1}{2} gH^2 \right)_x = 0.$$

As can be readily seen, for smooth solutions an equivalent formulation is obtained by further algebraic manipulation to yield the variant form (1.4) and (1.5). Finally, we turn to the conservation of energy. Total mechanical energy in the control volume is expressed

as

$$\begin{aligned} \frac{d}{dt} \int_{x_1}^{x_2} \int_0^{h+\eta} \rho \left(\frac{1}{2} \tilde{v}^2 + gz \right) dz dx \\ = \left[\int_0^{h+\eta} \rho \left(\frac{1}{2} \tilde{v}^2 + gz \right) \tilde{v} dz + \int_0^{h+\eta} \rho (h + \eta - z) \tilde{v} dz \right]_{x_2}^{x_1} \end{aligned}$$

Substituting (1.3) and integrating in the z -direction gives

$$\begin{aligned} \int_{x_1}^{x_2} \left(\frac{\Gamma}{2} uH^2 + \frac{\Gamma^2}{6} H^3 + \frac{1}{2} u^2H + \frac{1}{2} gH^2 \right)_t \\ + \left(\frac{3\Gamma}{4} u^2H^2 + \frac{\Gamma}{2} gH^3 + \frac{\Gamma^2}{2} uH^3 + \frac{\Gamma^3}{8} H^4 + \frac{1}{2} u^3H + guH^2 \right)_x dx = 0. \end{aligned}$$

Dividing through by $(x_1 - x_2)$ and taking the limit as $(x_1 - x_2) \rightarrow 0$ yield the energy conservation equation

$$\begin{aligned} \left(\frac{\Gamma}{2} uH^2 + \frac{\Gamma^2}{6} H^3 + \frac{1}{2} u^2H + \frac{1}{2} gH^2 \right)_t \\ + \left(\frac{3\Gamma}{4} u^2H^2 + \frac{\Gamma}{2} gH^3 + \frac{\Gamma^2}{2} uH^3 + \frac{\Gamma^3}{8} H^4 + \frac{1}{2} u^3H + guH^2 \right)_x = 0, \end{aligned}$$

which is the same as (1.6).

3. Mathematical description of the flow properties

We provide a discussion on the flow properties associated with waves propagation in shallow water in the presence of linear shear. The characteristics in this case are found by first putting the equation in characteristic form. In conservative variables $\mathbf{U} = (H, u)^T$, (1.4) and (1.5) are expressed in matrix notation as

$$\mathbf{U}_t + \mathbf{F}(\mathbf{U})_x = 0, \quad (3.1)$$

where $\mathbf{F}(\mathbf{U})_x = \mathbf{F}'(\mathbf{U})\mathbf{U}_x$. The flux Jacobian $\mathbf{F}'(\mathbf{U})$ is

$$\mathbf{F}'(\mathbf{U}) = \begin{pmatrix} \Gamma H + u & H \\ 1 & u \end{pmatrix}. \quad (3.2)$$

The eigenvalues of the Jacobian matrix are

$$\begin{aligned} \lambda_- = u + \frac{1}{2} \Gamma H - \sqrt{H + \left(\frac{1}{2} \Gamma H \right)^2} \quad \text{and} \\ \lambda_+ = u + \frac{1}{2} \Gamma H + \sqrt{H + \left(\frac{1}{2} \Gamma H \right)^2}, \end{aligned} \quad (3.3)$$

with $\lambda_- < \lambda_+$ for $H \neq 0$ so that the system is strictly hyperbolic. The corresponding right eigenvectors

$$\begin{aligned} r_- = \begin{pmatrix} 1 \\ -\frac{1}{2} \Gamma - \frac{1}{H} \sqrt{H + \left(\frac{1}{2} \Gamma H \right)^2} \end{pmatrix} \quad \text{and} \\ r_+ = \begin{pmatrix} 1 \\ -\frac{1}{2} \Gamma + \frac{1}{H} \sqrt{H + \left(\frac{1}{2} \Gamma H \right)^2} \end{pmatrix}, \end{aligned} \quad (3.4)$$

are linearly independent and therefore, span the eigenspace in the (H, u) -plane. Both characteristic fields are genuinely nonlinear with

$$\begin{aligned} \nabla \lambda_-(H, u) \cdot r_-(H, u) = -\frac{6gH + 2\Gamma^2 H^2}{\sqrt{4gH + \Gamma^2 H^2}} < 0 \\ \nabla \lambda_+(H, u) \cdot r_+(H, u) = +\frac{6gH + 2\Gamma^2 H^2}{\sqrt{4gH + \Gamma^2 H^2}} > 0. \end{aligned} \quad (3.5)$$

It is well-known that a traveling hydraulic jump over a flat bottom obeys mass conservation and momentum conservation. To describe the relation between the state variables on each side of the jump, we assume that the discontinuity is located at the bore

front. If we consider two constant states $(H, u) = (H_L, u_L)$ and $(H, u) = (H_R, u_R)$, then we obtain from (1.1) and (1.2) the Rankine–Hugoniot conditions

$$-s[H] + \left[\frac{\Gamma}{2} H^2 + uH \right] = 0, \quad (3.6)$$

$$-s \left[\frac{\Gamma}{2} H^2 + uH \right] + \left[\frac{\Gamma^2}{3} H^3 + \Gamma uH^2 + u^2 H + \frac{1}{2} gH^2 \right] = 0. \quad (3.7)$$

Define $[H] = H_R - H_L$ and $[u] = u_R - u_L$, where the subscripts L and R denote the left and right states of the hydraulic jump respectively. Then we can explicitly write

$$s(H_R - H_L) = \left(\frac{\Gamma}{2} H_R^2 + u_R H_R - \frac{\Gamma}{2} H_L^2 + u_L H_L \right),$$

$$s \left(\frac{\Gamma}{2} H_R^2 + u_R H_R - \frac{\Gamma}{2} H_L^2 + u_L H_L \right) = \left(\frac{\Gamma^2}{3} H_R^3 + \Gamma u_R H_R^2 + u_R^2 H_R \right. \\ \left. + \frac{1}{2} g H_R^2 - \frac{\Gamma^2}{3} H_L^3 + \Gamma u_L H_L^2 + u_L^2 H_L + \frac{1}{2} g H_L^2 \right).$$

The shock speed, s , satisfies the Lax entropy condition [26,30]

$$\lambda_-(H_R, v_R) < s < \lambda_-(H_L, v_L), \quad s < \lambda_+(H_R, v_R), \quad (3.8)$$

for a 1-shock and

$$\lambda_+(H_R, v_R) < s < \lambda_+(H_L, v_L), \quad s > \lambda_-(H_L, v_L), \quad (3.9)$$

for a 2-shock and is expressed as

$$s = \frac{\frac{\Gamma}{2} H_R^2 + u_R H_R - \frac{\Gamma}{2} H_L^2 + u_L H_L}{H_R - H_L}$$

$$= \frac{\frac{\Gamma^2}{3} H_R^3 + \Gamma u_R H_R^2 + u_R^2 H_R + \frac{1}{2} g H_R^2 - \frac{\Gamma^2}{3} H_L^3 + \Gamma u_L H_L^2 + u_L^2 H_L + \frac{1}{2} g H_L^2}{\frac{\Gamma}{2} H_R^2 + u_R H_R - \frac{\Gamma}{2} H_L^2 + u_L H_L}. \quad (3.10)$$

Considering the expressions on both sides of the last equality, we obtain

$$(u_R - u_L)^2 = \frac{\Gamma^2}{12 H_L H_R} (H_R - H_L)^4 + \Gamma (H_R - H_L) (u_L - u_R) \\ + \frac{g}{2} (H_R + H_L) (H_R - H_L)^2$$

Simplifying this expression further gives the relation

$$u_R - u_L = \frac{\Gamma}{2} (H_R - H_L) \\ \times \left(-1 \pm \sqrt{\frac{1}{3} + \frac{1}{H_L} \left(\frac{H_R}{3} + \frac{2g}{\Gamma^2} \right) + \frac{1}{H_R} \left(\frac{H_L}{3} + \frac{2g}{\Gamma^2} \right)} \right). \quad (3.11)$$

It is obvious to see that the relation between the states u_R and u_L is either positive or negative and is dependent on the fluid depths H_R and H_L on each side of the shock. It shall be shown how the state variables H, u and s are related on each side of the hydraulic jump but firstly, we write the shock speed in terms of the above expression. Substituting this relation into Eq. (3.10) gives

$$s = u_R + \frac{\Gamma}{2} H_R \pm \frac{\Gamma}{2} H_L \sqrt{\frac{1}{3} + \frac{1}{H_L} \left(\frac{H_R}{3} + \frac{2g}{\Gamma^2} \right) + \frac{1}{H_R} \left(\frac{H_L}{3} + \frac{2g}{\Gamma^2} \right)}$$

$$= u_L + \frac{\Gamma}{2} H_L \pm \frac{\Gamma}{2} H_R \sqrt{\frac{1}{3} + \frac{1}{H_L} \left(\frac{H_R}{3} + \frac{2g}{\Gamma^2} \right) + \frac{1}{H_R} \left(\frac{H_L}{3} + \frac{2g}{\Gamma^2} \right)}. \quad (3.12)$$

Schematics of shocks of the first and the second families and the characteristic curves are shown in Figs. 2 and 3. As mentioned earlier, a discontinuity propagating over a flat-bottom at a speed s , given in (3.12), must respect mass conservation. In what follows, a mathematical expression representing mass conservation through the discontinuity is obtained in terms of the shock speed. From Eq. (3.6) we get

$$\mu \equiv \frac{\Gamma}{2} H_R^2 + (u_L - s) H_L = \frac{\Gamma}{2} H_L^2 + (u_R - s) H_R. \quad (3.13)$$

Inserting the shock speed in (3.12) gives

$$\mu = \mp \frac{\Gamma}{2} H_L H_R \sqrt{\frac{1}{3} + \frac{1}{H_L} \left(\frac{H_R}{3} + \frac{2g}{\Gamma^2} \right) + \frac{1}{H_R} \left(\frac{H_L}{3} + \frac{2g}{\Gamma^2} \right)}. \quad (3.14)$$

In a similar manner, conservation of momentum through the hydraulic jump is derived from (3.7) as

$$\left(\frac{\Gamma}{2} H_R^2 + u_R H_R \right) (u_R - c) + \frac{\Gamma}{2} u_R H_R^2 + \frac{\Gamma}{3} H_R^3 + \frac{1}{2} g H_R^2$$

$$= \left(\frac{\Gamma}{2} H_L^2 + u_L H_L \right) (u_L - c) + \frac{\Gamma}{2} u_L H_L^2 + \frac{\Gamma}{3} H_L^3 + \frac{1}{2} g H_L^2.$$

Inserting (3.13) into the above expression leads to

$$\mu \left(\frac{\Gamma}{2} H_R + u_R \right) + \frac{\Gamma}{12} H_R^3 + \frac{1}{2} g H_R^2$$

$$= \mu \left(\frac{\Gamma}{2} H_L + u_L \right) + \frac{\Gamma}{12} H_L^3 + \frac{1}{2} g H_L^2. \quad (3.15)$$

The Rankine–Hugoniot condition for Eq. (1.6) is

$$-s \left[\frac{\Gamma^2}{6} H^3 + \frac{\Gamma}{2} uH^2 + \frac{1}{2} u^2 H + \frac{1}{2} gH^2 \right]$$

$$+ \left[\frac{\Gamma^3}{8} H^4 + \frac{\Gamma^2}{2} uH^3 + \frac{3\Gamma}{4} u^2 H^2 + \frac{\Gamma}{2} gH^3 + \frac{1}{2} u^3 H + guH^2 \right] = 0. \quad (3.16)$$

The mechanical energy associated with the above Rankine–Hugoniot condition dissipates in the discontinuity. Out of the discontinuity where the solution is smooth, the mechanical energy is conserved. The hydraulic jump can therefore, be interpreted as heat dump which absorbs the excess energy of the fluid. We derive in what follows a mathematical expression that represents the energy loss. In order words, we show that an admissible shock wave solution that satisfies the Rankine–Hugoniot condition in (3.16) dissipates mechanical energy. From (3.16) we have

$$\Delta E = E_R - E_L, \quad (3.17)$$

where

$$E_R = \left(\frac{\Gamma^3}{6} H_R^4 + \frac{\Gamma^2}{2} u_R H_R^3 - s \frac{\Gamma^2}{6} H_R^3 + \frac{3\Gamma}{4} u_R^2 H_R^2 + \right. \\ \left. \frac{\Gamma}{2} g H_R^3 - s \frac{\Gamma}{2} u_R H_R^2 + \frac{1}{2} u_R^3 H_R + g u_R H_R^2 - s \frac{1}{2} u_R^2 H_R - s \frac{1}{2} g H_R^2 \right), \quad (3.18)$$

and

$$E_L = \left(\frac{\Gamma^3}{6} H_L^4 + \frac{\Gamma^2}{2} u_L H_L^3 - s \frac{\Gamma^2}{6} H_L^3 + \frac{3\Gamma}{4} u_L^2 H_L^2 + \right. \\ \left. \frac{\Gamma}{2} g H_L^3 - s \frac{\Gamma}{2} u_L H_L^2 + \frac{1}{2} u_L^3 H_L + g u_L H_L^2 - s \frac{1}{2} u_L^2 H_L - s \frac{1}{2} g H_L^2 \right). \quad (3.19)$$

E_R and E_L represent the energy on the right and the left of the hydraulic jump. It is obvious from (3.12) that the discontinuity can propagate either to the right or to the left. For a right going shock for instance, E_R represents the mechanical energy after the discontinuity while E_L symbolizes the energy before the discontinuity. Through the jump, we have

$$\Delta E = \left(\frac{1}{2} u_R^2 + \frac{1}{2} g H_R \right) (u_R - s) H_R + \frac{\Gamma}{2} H_R^2$$

$$- \left(\frac{1}{2} u_L^2 + \frac{1}{2} g H_L \right) (u_L - s) H_L + \frac{\Gamma}{2} H_L^2$$

$$+ \frac{\Gamma^3}{8} (H_R^4 - H_L^4) + \frac{\Gamma^2}{2} (u_R H_R^3 - u_L H_L^3)$$

$$- \frac{s \Gamma^2}{6} (H_R^3 - H_L^3) + \frac{\Gamma}{2} (u_R^2 H_R^2 - u_L^2 H_L^2)$$

$$- \frac{s \Gamma}{2} (u_R H_R^2 - u_L H_L^2) + \frac{g \Gamma}{4} (H_R^3 - H_L^3) + \frac{g}{2} (u_R H_R^2 - u_L H_L^2).$$

Applying the expressions for mass conservation and momentum conservation through the discontinuity (see Eqs. (3.13) and (3.15))

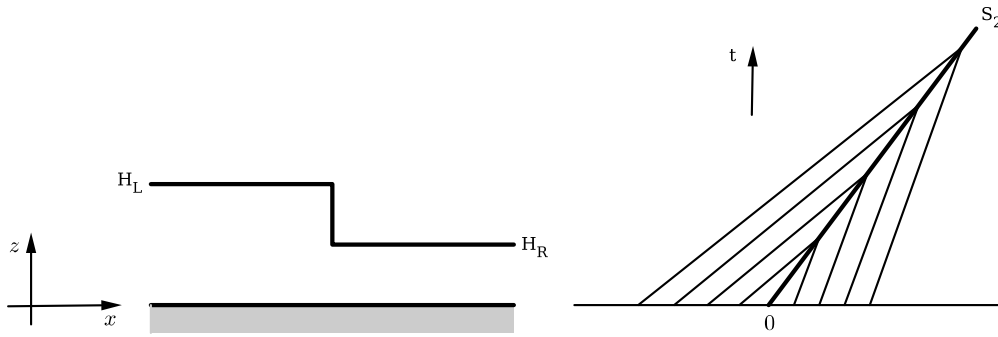


Fig. 2. Schematic representation of a linear shear flow over an even bottom. S_2 is a shock of the second family.

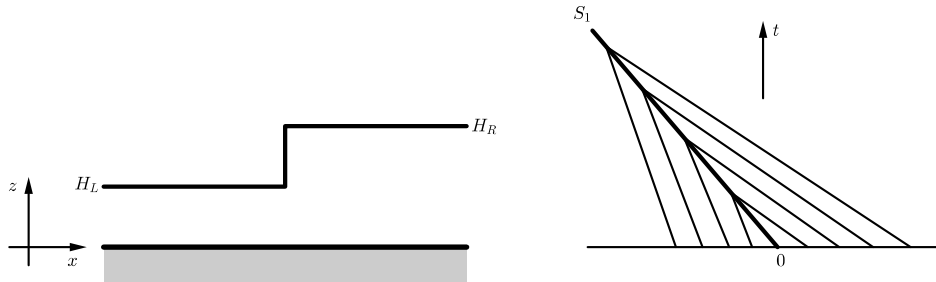


Fig. 3. Schematic representation of a linear shear flow over an even bottom. S_1 is a shock of the first family.

give

$$\Delta E = \frac{\mu}{2} \left(((u_R - s) + \frac{\Gamma}{2} H_R)^2 - ((u_L - s) + \frac{\Gamma}{2} H_L)^2 + \frac{\Gamma^2}{4} (H_R^2 - H_L^2) + 2g(H_R - H_L) \right).$$

By focusing on the first two terms on the right hand side, it is noted from (3.13) that

$$\begin{aligned} ((u_R - s) + \frac{\Gamma}{2} H_R)^2 &= \left(\frac{\Gamma}{2} H_L \right)^2 \left(\frac{1}{3} + \frac{1}{H_L} \left(\frac{H_R}{3} + \frac{2g}{\Gamma^2} \right) + \frac{1}{H_R} \left(\frac{H_L}{3} + \frac{2g}{\Gamma^2} \right) \right), \\ ((u_L - s) + \frac{\Gamma}{2} H_L)^2 &= \left(\frac{\Gamma}{2} H_R \right)^2 \left(\frac{1}{3} + \frac{1}{H_L} \left(\frac{H_R}{3} + \frac{2g}{\Gamma^2} \right) + \frac{1}{H_R} \left(\frac{H_L}{3} + \frac{2g}{\Gamma^2} \right) \right). \end{aligned}$$

Substituting these relations into the preceding expression for the energy loss, we get

$$\Delta E = -\mu(H_R - H_L)^3 \left(\frac{\Gamma^2(H_L + H_R) + 6g}{24H_L H_R} \right). \tag{3.20}$$

Notice firstly, that the fractional term on the right hand side is strictly positive. It is noted also that $H_L \neq H_R$ if and only if $v_L \neq v_R$. Consequently, the mechanical energy loss through the discontinuity requires that

$$\mu(H_R - H_L)^3 > 0. \tag{3.21}$$

This inequality together with mass conservation through the discontinuity (see Eq. (3.13)) and the total velocity component (1.3) give the following conditions

$$\begin{aligned} H_R > H_L &\iff v_R > s \text{ and } v_L > s, \\ H_R < H_L &\iff v_R < s \text{ and } v_L < s. \end{aligned} \tag{3.22}$$

The first condition in (3.22) simply describes a hydraulic jump in which the fluid depth on the right is larger than that on the left. In this case, the propagating shock speed s is greater than the fluid velocities on both sides of the jump. In other words, we say that

the shear flow traveling at speed v_L hit the shock from the left and become mitigated as they emerge from the shock with traveling speed v_R . The same explanation holds for the second condition. From the mass conservation through the hydraulic jump given in (3.13) and Eqs. (3.11) and (3.12), it is found that the relation

$$v_R - v_L = -\frac{\mu(H_R - H_L)}{H_R H_L}, \tag{3.23}$$

holds. Applying the strictly positive inequality in (3.21) gives the relation

$$v_R < v_L. \tag{3.24}$$

In Fig. 3, a propagating 1-shock moving to the left is shown where the shock speed is larger than the characteristic speeds on left side of the shock but lower than those on the right. The characteristics emanating from $x > 0$ and $x < 0$ propagate into the shock. The conditions (3.22) and (3.24) play an important role in analyzing the Rankine–Hugoniot jump condition for the shear flow. In fact it can be shown that the shock given in (3.12) satisfies these conditions. For $H_R > H_L$, we have a 1-shock, $s = S_1$, such that

$$\begin{aligned} v_R > u_R + \frac{\Gamma}{2} H_R > u_R + \frac{\Gamma}{2} H_L \\ - \sqrt{\frac{1}{3} + \frac{1}{H_L} \left(\frac{H_R}{3} + \frac{2g}{\Gamma^2} \right) + \frac{1}{H_R} \left(\frac{H_L}{3} + \frac{2g}{\Gamma^2} \right)} = S_1. \end{aligned}$$

The inequality $v_L > s$ is proved in like manner and justifies the first condition in (3.22) Similarly, $H_R < H_L$ gives a 2-shock, $s = S_2$, satisfying

$$\begin{aligned} v_R < u_R + \frac{\Gamma}{2} H_R + \frac{\Gamma}{2} H_L \\ < u_R + \frac{\Gamma}{2} H_R \\ + \frac{\Gamma}{2} H_L \sqrt{\frac{1}{3} + \frac{1}{H_L} \left(\frac{H_R}{3} + \frac{2g}{\Gamma^2} \right) + \frac{1}{H_R} \left(\frac{H_L}{3} + \frac{2g}{\Gamma^2} \right)} = S_2. \end{aligned}$$

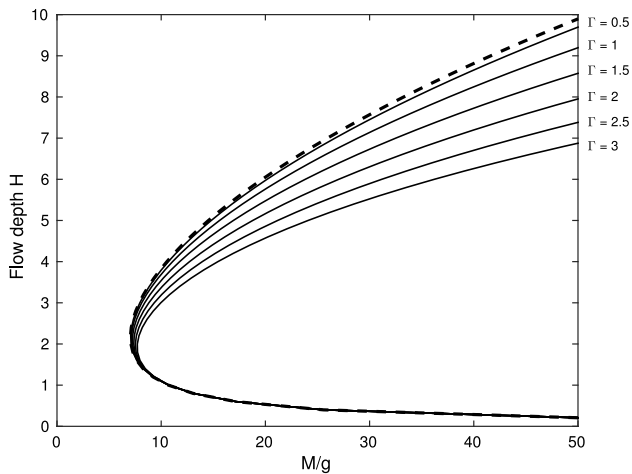


Fig. 4. The momentum function M/g is plotted against the flow depth for various strengths of vorticity. The dashed line shows the irrotational case $\Gamma = 0$. The other curves show the respective cases of the strengths of the vorticity Γ .

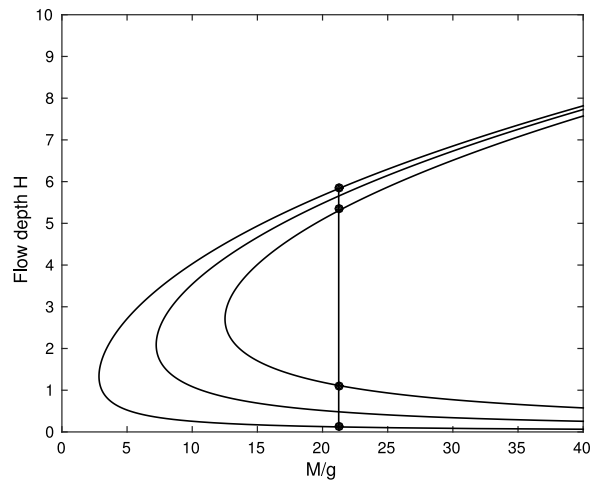


Fig. 5. The momentum function M/g is plotted against the flow depth H for constant vorticity $\Gamma = 1.5$ and different values of the flow rate per unit width Δ .

4. Steady state solution

We analyze the hydraulic jump by using the Froude number which is defined in such a way that it takes into account the average flow velocity over the entire fluid depth. In dimensionless variables, the depth averaging integral gives

$$Fr = \frac{\frac{1}{H} \int_0^H U + u \, dz}{\sqrt{gH}}$$

By using (1.3), the Froude number simplifies to

$$Fr = \frac{u + \frac{\Gamma}{2}H}{\sqrt{gH}}$$

The analysis is based on the hypothesis that the hydraulic jump is stationary and that the velocity and water depth increase across the jump. If we let Δ represent the volume flow rate per unit width, then the conservation of mass necessitates that

$$\Delta = u_L H_L + \frac{\Gamma}{2} H_L^2 = u_R H_R + \frac{\Gamma}{2} H_R^2, \tag{4.1}$$

be satisfied. Using the concept of momentum conservation explained above, an expression for the momentum conservation across the discontinuity is obtained in the form

$$\begin{aligned} \frac{\Gamma^2}{3} H_L^3 + \Gamma u_L H_L^2 + u_L^2 H_L + \frac{1}{2} g H_L^2 \\ = \frac{\Gamma^2}{3} H_R^3 + \Gamma u_R H_R^2 + u_R^2 H_R + \frac{1}{2} g H_R^2. \end{aligned} \tag{4.2}$$

In particular, if we define $M = \frac{\Gamma^2}{3} H^3 + \Gamma u H^2 + u^2 H + \frac{1}{2} g H^2$ the quantity M/g is the analogue of the momentum function used in hydraulic engineering. Since M needs to be preserved through a stationary jump, for a given volume flow rate per unit width Δ , one can find the conjugate flow depths by plotting the curve

$$M = \frac{1}{12} \Gamma^2 H^3 + \frac{\Delta^2}{H} + \frac{1}{2} g H^2.$$

Such a plot is shown in Fig. 4 for $\Delta = 10$ and a variety of background vorticities ranging from $\Gamma = 0$ to $\Gamma = 3$. On the other hand, Fig. 5 shows the graphs for a fixed $\Gamma = 1.5$ but for a variety of values of Δ .

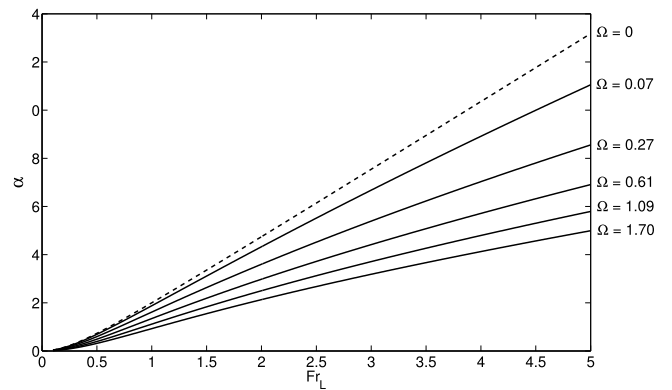


Fig. 6. The ratio of right to left Froude numbers α plotted against the left Froude number Fr_L for various strengths of vorticity Ω . The dashed curve depicts the irrotational case.

If we substitute the expression for Δ into relation (4.2), then we get

$$\Delta^2 \left(\frac{1}{H_R} - \frac{1}{H_L} \right) = \frac{\Gamma^2}{12} (H_L^3 - H_R^3) + \frac{1}{2} g (H_L^2 - H_R^2). \tag{4.3}$$

Substituting the expression for the Froude number stated above and carrying out further algebraic simplification gives the cubic function

$$\frac{\Gamma^2}{6g} H_L \alpha^3 + \left(1 + \frac{\Gamma^2}{6g} H_L \right) \alpha^2 + \left(1 + \frac{\Gamma^2}{6g} H_L \right) \alpha - 2Fr_L^2 = 0, \tag{4.4}$$

where $\alpha = H_R/H_L$ is the ratio of depths. Note that the strength of vorticity depends on the non-dimensional parameter $\Omega = H_L \Gamma^2 / 6g$, so that we can write the equation in the final form

$$\Omega \alpha^3 + (1 + \Omega) \alpha^2 + (1 + \Omega) \alpha - 2Fr_L^2 = 0. \tag{4.5}$$

The cubic equation can be solved for any value of Ω . Fig. 6 shows a plot of α as a function of Fr_L for a number of values of the vorticity Γ . It is apparent that larger values of Ω have the effect of moderating the strength of the hydraulic jump.

Acknowledgment

This research was supported by the Research Council of Norway under grant no. 239033/F20.

References

- [1] T. Colin, F. Dias, J.-M. Ghidaglia, On rotational effects in the modulations of weakly nonlinear water waves over finite depth, *Eur. J. Mech. B Fluids* 14 (1995) 775–793.
- [2] R. Thomas, C. Kharif, M. Manna, A nonlinear Schrödinger equation for water waves on finite depth with constant vorticity, *Phys. Fluids* 24 (2012) 127102.
- [3] A. Ali, H. Kalisch, Reconstruction of the pressure in long-wave models with constant vorticity, *Eur. J. Mech. B Fluids* 37 (2013) 187–194.
- [4] W. Choi, Strongly nonlinear long gravity waves in uniform shear flows, *Phys. Rev. E* 68 (2003) 026305.
- [5] A.F. Teles da Silva, D.H. Peregrine, Steep, steady surface waves on water of finite depth with constant vorticity, *J. Fluid Mech.* 195 (1988) 281–302.
- [6] R. Ribeiro, P.A. Milewski, A. Nachbin, Flow structure beneath rotational water waves with stagnation points, *J. Fluid Mech.* 812 (2017) 792–814.
- [7] A. Senthilkumar, H. Kalisch, Wave breaking in the KdV equation on a flow with constant vorticity, *Eur. J. Mech. B Fluids*, <https://doi.org/10.1016/j.euromechflu.2017.12.006>.
- [8] B.L. Segal, D. Moldabayev, H. Kalisch, B. Deconinck, Explicit solutions for a long-wave model with constant vorticity, *Eur. J. Mech. B Fluids* 65 (2017) 247–256.
- [9] E. Terrile, M. Brocchini, K.H. Christensen, J.T. Kirby, Dispersive effects on wave–current interaction and vorticity transport in nearshore flows: a GLM approach, *Phys. Fluids* 20 (2008) 036602.
- [10] C.W. Curtis, H. Kalisch, Vortex dynamics in nonlinear free surface flows, *Phys. Fluids* 29 (2017) 032101.
- [11] J. Shatah, S. Walsh, C. Zeng, Travelling water waves with compactly supported vorticity, *Nonlinearity* 26 (2013) 1529.
- [12] P. Karageorgis, Dispersion relation for water waves with non-constant vorticity, *Eur. J. Mech. B Fluids* 34 (2012) 7–12.
- [13] A. Castro, D. Lannes, Fully nonlinear long-wave models in the presence of vorticity, *J. Fluid Mech.* 759 (2014) 642–675.
- [14] A. Constantin, E. Varvaruca, Steady periodic water waves with constant vorticity: Regularity and local bifurcation, *Arch. Ration. Mech. Anal.* 199 (2011) 33–67.
- [15] J. Escher, D. Henry, B. Kolev, T. Lyons, Two-component equations modelling water waves with constant vorticity, *Ann. Mat. Pura Appl.* 195 (2016) 249–271.
- [16] R. Ivanov, Two-component integrable systems modelling shallow water waves: the constant vorticity case, *Wave Motion* 46 (2009) 389–396.
- [17] R.S. Johnson, The Camassa–Holm equation for water waves moving over a shear flow, *Fluid Dyn. Res.* 33 (2003) 97–111.
- [18] Y. Kang, J.M. Vanden-Broeck, Gravity-capillary waves in the presence of constant vorticity, *Eur. J. Mech. B Fluids* 19 (2000) 253–268.
- [19] C.W. Curtis, K.L. Oliveras, T. Morrison, Shallow waves in density stratified shear currents, *Eur. J. Mech. B Fluids* 61 (2016) 100–111.
- [20] I.G. Jonsson, Wave–current interactions, in: Le Mehaute, Hanes (Eds.), *The Sea*, 9(a), Ocean Eng. Sc., Wiley, New York, 1990, pp. 65–120.
- [21] I.G. Jonsson, O. Brink-Kjaer, G.P. Thomas, Wave action and set-down for waves on a shear current, *J. Fluid Mech.* 87 (1978) 401–416.
- [22] M. Bjørnstad, H. Kalisch, Shallow water dynamics on linear shear flows and plane beaches, *Phys. Fluids* 29 (2017) 073602.
- [23] V.M. Hur, Shallow water models with constant vorticity, *Eur. J. Mech. B Fluids*, <https://doi.org/10.1016/j.euromechflu.2017.06.001>.
- [24] C. Kharif, M. Abid, J. Touboul, Rogue waves in shallow water in the presence of a vertically sheared current, *J. Ocean Eng. Mar. Energy* 3 (2017) 301–308.
- [25] G. Richard, S. Gavriluk, The classical hydraulic jump in a model of shear shallow-water flows, *J. Fluid Mech.* 725 (2013) 492–521.
- [26] H. Holden, N.H. Risebro, *Front Tracking for Hyperbolic Conservation Laws*, Springer, New York, 2002.
- [27] R.J. LeVeque, *Finite Volume Methods for Hyperbolic Problems*, Cambridge University Press, 2002.
- [28] G.B. Whitham, *Linear and Nonlinear Waves*, Wiley, New York, 1974.
- [29] H. Kalisch, D. Mitrovic, V. Teyekpiti, Delta shock waves in shallow water flow, *Phys. Lett. A* 381 (2017) 1138–1144.
- [30] P.D. Lax, Hyperbolic systems of conservation laws II, *Comm. Pures Appl. Math.* 10 (1957) 537–566.